J Electr Eng Technol.2016; 11(6): 1693-1699
http://dx.doi.org/10.5370/JEET.2016.11.6.1693

ISSN(Print) 1975-0102
ISSN(Online) 2093-7423

Research on Oscillation Character of Six-Phase Fractional-Slot Concentrated-Winding Permanent Motor with Different Slot-Pole Match

Qiao Ming-zhong*, Zhu Yong-xin†, Liang Jing-hui* and Li Geng*

Abstract – The oscillation character of permanent magnetic motor is highly related to its slot-pole match. By calculating air-gap magnet field and radial electromagnetic force of 6-phase fractional-slot concentrated-winding permanent magnetic motor with slot–pole match of 48/44, 48/46, 48/50 and 48/52 under no load and load status, oscillation character of permanent magnetic motor is analyzed. A 20kW prototype with 48 slots and 44 poles is designed. With many sensors attaching to the corresponding parts, oscillatory acceleration is measured, and spectrum of oscillation frequency is recorded as well. The experiment results give proof to the analysis method for permanent magnetic motor oscillation in this paper.

Keywords: Fractional-slot, Concentrated-winding, Radial electromagnetic force, Slot-pole match

1. Introduction

Low-speed motor usually has many poles, and the number of q, which means slots under each pole and each phase, could not be too big, or external diameter of stator may increase, bringing difficulty in motor manufacture. If q takes a smaller integer, total slot number of stator could be fewer, but cogging harmonics would be enhanced in amplitude, which will increase harmonic proportion in back EMF[1]. By using fractional-slot winding, coils of the same phase winding can be placed under different magnetic poles. This kind of assignment could weaken harmonics and obtain more sinusoidal back EMF waves. Besides, in concentrated fractional-slot winding (winding pitch y=1), coils can be directly wrapped around one tooth, and the length of winding ends can be decreased [2, 3], and motor materials can be saved and thermal loss of motor can be reduced [4-7]. Consequently, fractional-slot concentrated-winding PM motor is very suitable for occasions with insufficient space, such as ship, locomotive, etc. Fractional-slot concentrated-winding motor has better back EMF, but stator current may produce strong harmonic magneto motive force, which will cause intense oscillation and noise.

Motor oscillation and noise include three main kinds: oscillation and noise caused by electromagnetism, mechanics and air. Generally, air noise can be neglected as it is relatively small, especially in the condition that external fan is not used and speed is not very fast. Mechanical oscillation and noise are mainly related to mechanical installation technology of bearing and electric brush, and it can be effectively weakened by improving processing and technology level. Electromagnetic vibration and noise are mainly caused by electromagnetic force of motor itself. Tangential component of electromagnetic force chiefly rotates the rotor, and radial component mainly makes stator deform and vibrate, and thus causes oscillation and noise. Generally speaking, electromagnetic vibration is the main source of motor's oscillation and noise [8].

Literature [8] studied 3-phase PM motors with 12 slots and 8 poles, 24 slots and 8 poles and 12 slots and 10 poles, and analyzed the influence from radial force harmonic to oscillation, coming to the conclusion that radial force with smaller order has bigger influence to oscillation. Literature [9] studied 3-phase PM motors with slot - pole matches of 18/6, 9/6, 12/8, 15/10 and 12/10 under load and no-load condition, and analyzed radial and tangential moment on its stator-tooth, and calculated noise intensity under different slot-pole matches. Literature [10] calculated integral-slot and fractional-slot linear PM motor's moment pulsation, and concluded that it can be restrained through fractional-slot and optimized control algorithm. Literature [11] analyzed oscillatory force of 3-phase fractional-slot concentrated-winding PM brushless motor with different slot-pole combinations, and the 12/10 match possessed maximum force. Literature [12] compares oscillation and noise of fractional-slot concentrated-winding PM motor with slot-pole match of 8/12 and 10/12. Literature [13] researched on a 3-phase 44-pole 48-slot fractional-slot concentrated-winding PM motor, and calculated the influence from PM length and stator tooth to motor oscillation. All these studies above have much academic value, but most of these articles are based on low power rather than high power low-speed motors.

This paper focuses on high power low-speed 6-phase fractional-slot concentrated-winding PM motor, which is suitable to be applied to ship and launches, and analyzes

† Corresponding Author: Dept. of Electrical Engineering, Naval University of Engineering, China. (gagaga92@163.com)
* Dept. of Electrical Engineering, Naval University of Engineering, China. ({qiaomingzhong, liangjinghui04}@163.com, to-terabithia@live.cn)
Received: December 7, 2015; Accepted: May 27, 2016

air gap magnetic density and radial electromagnetic force of this kind of PM motor, with slot-pole matches of 48/44, 48/46, 48/50 and 48/52. A 20kW 6-phase fractional-slot concentrated-winding PM motor prototype with 48 slots and 44 poles is designed and manufactured, and its oscillatory characteristics are experimentally studied.

2. Electromagnetic Oscillation Analysis of PM Synchronous-motor

Radial electromagnetic force is the main cause of electromagnetic oscillation in PM synchronous motor [8]. Therefore, the influence from radial electromagnetic force to PM synchronized motor is mainly analyzed in this paper. When the motor is working, alternative radial electromagnetic force in air gap affects stator and rotor iron core, and makes them deform periodically, and oscillation is caused. When the frequency of radial electromagnetic force comes close to or equals to natural frequency of motor, resonance will appear, and the amplitude of oscillation and noise caused by it will be greatly enhanced.

According to Maxwell Rule, the radial electromagnetic force in motor can be described as:

$$F_r = \frac{1}{2\mu}(B_r^2 - B_t^2) \tag{1}$$

In equation (1), F_r means radial Maxwell electromagnetic force, μ means air gap magnetic inductivity, B_r *and* B_t respectively means air gap radial and tangential magnetic density.

Neglecting the influence caused by motor frame, stator can be simplified to a single ring form which only contains iron core. Only yoke deformation of stator iron core is considered, and stator teeth and windings are additional weight. The static deformation of stator iron core caused by radial electromagnetic force can be expressed as follow:

$$d_s = \frac{3}{4}\frac{F_r}{E}\left(\frac{D_e}{h_e}\right)^3 \frac{l}{\gamma^3}\times 10^6 \tag{2}$$

In the expressing, F_r refers to radial force; l refers to the distance between iron core beam fulcrums; E refers to iron core elastic modulus; D_e refers to average diameter of stator iron core yoke; h_e means stator iron core yoke height; and γ means force wave power.

When the order of radial electromagnet force is 0, expression (2) can be simplified to:

$$d_s = \frac{F_r}{E}\frac{D_e}{h_e}\times 10^6 \tag{3}$$

For the 0th order force, stator radial vibration is balanced, and its natural frequency can be expressed as:

$$f_{\gamma 0} = \frac{1}{\pi D_e}\sqrt{\frac{E}{\rho_i \Delta_0}} \tag{4}$$

ρ_i is density of iron core; Δ_0 is mass addition coefficient corresponding to 0th force; $\Delta_0 = 1 + \frac{G_t + G_w}{G_e}$, G_t, G_w, and G_e separately represent mass of stator teeth, windings and yoke.

When force order is 1, iron core oscillation is affected by periodical unilateral magnetic force. Natural frequency of this kind of oscillation is:

$$f_{\gamma 1} = f_{\gamma 0}\sqrt{\frac{2}{1+\frac{1}{\sqrt{3}}\frac{h_e \Delta_\gamma}{\Delta_0 D_e}}} \tag{5}$$

When γ, which means the order of radial electromagnetic force, is more than 1, bending deformation will happen to the stator iron core, and expression of natural frequency considering bending oscillation is:

$$f_\gamma = f_{\gamma 0}\frac{i\gamma\left(\gamma^2 - 1\right)}{\sqrt{\gamma^2 + 1}}\phi_\gamma \tag{6}$$

In which,

$$\phi_\gamma = \frac{1}{\sqrt{1+\frac{i^2\left(\gamma - 1^2\right)\left[\gamma^2\left(4+\frac{\Delta_\gamma}{\Delta_0}\right)+3\right]}{\gamma^2+1}}}$$

$$i = \frac{1}{\sqrt{3}}\frac{h_e}{D_e}$$

When iron core vibration frequency caused by radial electromagnetic force is close to or equals to natural frequency, resonance will be caused and the deformation amount of iron core will increase. The real deformation, which means displacement amplitude of the stator core vibration, is as follow:

$$d = \frac{d_s}{\sqrt{\left[1-\left(f/f_{\gamma 0}\right)^2\right]^2 + \left[\left(f/f_{\gamma 0}\right)\frac{c}{\pi}\right]^2}} \tag{7}$$

And c is damping coefficient.

From the analysis above, motor oscillation is proportional to radial electromagnetic force, and is in inverse proportion to cubic of force order. When motor's

oscillation frequency is close or equal to natural frequency, vibration will be caused.

3. Electromagnetic Force Calculations Under Different Slot-Pole Matches

To calculate radial electromagnetic force of motor according to expression (1), air gap magnetic density should be calculated first. Air gap magnetic density is highly related to motor structure and saturation of every part. The analytic method is difficult to take every harmonic and saturation into account. 2-D Finite Element Method (FEM) is adapted in this paper to calculate magnetic field of motor.

3.1 Electromagnetic field analysis under different slot-pole matches

In order to analyze influence from different slot-pole matches to oscillation, analysis and calculation are conducted in four fractional-slot concentrated-winding PM motors, which has the slot–pole matches of 48/44, 48/46, 48/50 and 48/52. These four motors are all 6-phase PM synchronized with the power of 20kW and with the same structure parameters. Conditions that four motors meet with are shown in Table 1.

Fundamental magnetic fields produced by stator windings are equal; fundamental magnetic fields produced by rotors are equal; fundamental of back EMF are equal (fundamental peak is 306V); the average of electro-magnetic torques under rated current are equal.

Fig. 1 shows structures, no-load magnetic field distribution of four motors and half unit motor structure. Fig. 2 is no-load air gap magnetic density of four motors,

Table 1. Basic parameters of motors with different slot-pole match

Slot-pole match	Iron core length (mm)	Thickness of PM magnetizing (mm)	Conductors per slot	Maximum of stator current(A)
48/44	245	10	34	24
48/46	245	10	34	24
48/50	245	10	34	24
48/52	245	10	34	24

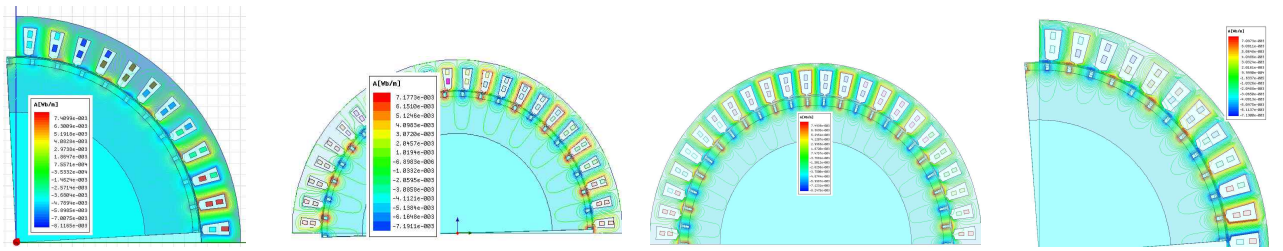

(a) 48-slot 44-pole motor (b) 48-slot 46-pole motor (c) 48-slot 50-pole motor (d) 48-slot 52-pole motor

Fig. 1. No load magnetic flux line of motors

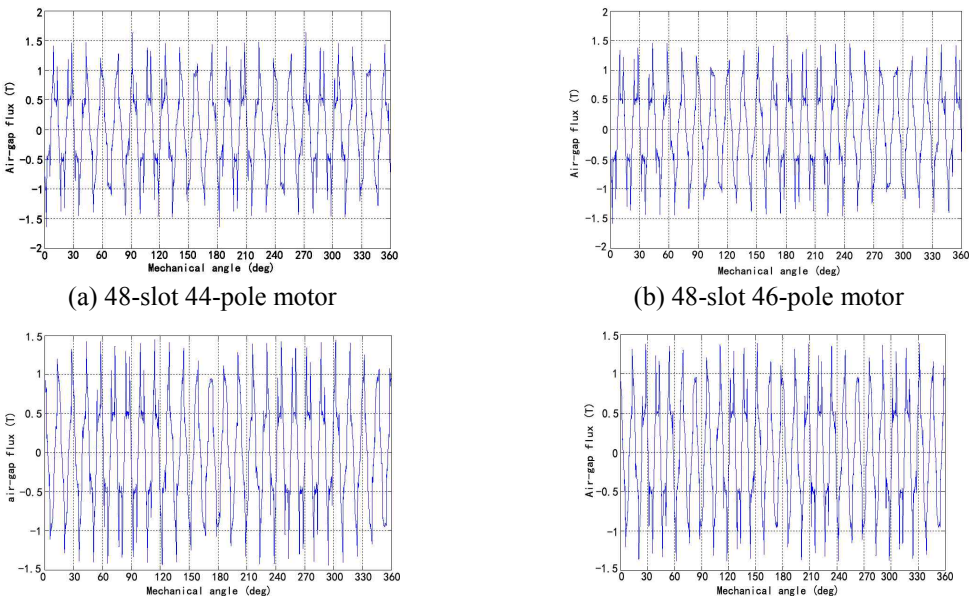

(a) 48-slot 44-pole motor (b) 48-slot 46-pole motor

(c) 48-slot 50-pole motor (d) 48-slot 52-pole motor

Fig. 2. No load air-gap induction of motors

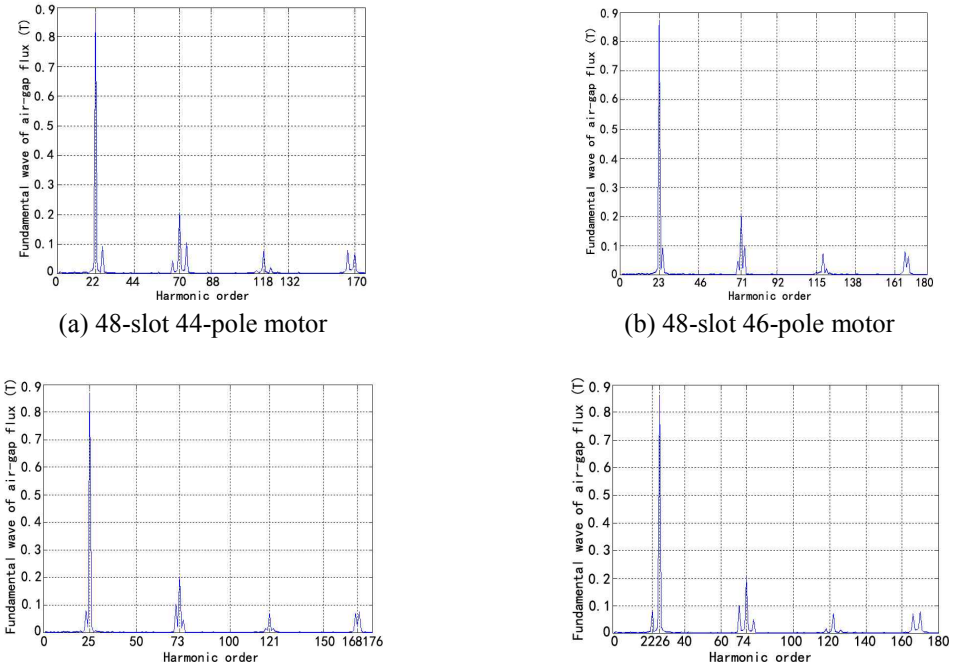

(a) 48-slot 44-pole motor (b) 48-slot 46-pole motor

(c) 48-slot 50-pole motor (d) 48-slot 52-pole motor

Fig. 3. Air-gap induction harmonic contents distribution of load motors

Table 2. Comparison of motor's oscillation with different slot-pole match

Slot-pole matches	Degree of radial force wave and average value of one period (KN/m^2)	Rated load air gap magnetic density harmonic distribution	No-load air gap magnetic density harmonic wave distribution (some moment)
48-slot 44-pole	4degree: 15.865 44degree: 151.7 (main wave) 48degree: 95.67; 52degree: 38.74 92degree: 67.93; 96degree: 74.26	22degree: 0.8798 T (main wave) 23degree: 2%; 26degree: 10.45% 70degree: 23.278% 74degree: 11.82%	22degree: 0.8985T (main wave) 23degree: 2.17% 26degree: 11.19% 70degree: 22.78% 74degree: 11.9%
48-slot 46-pole	2degree: 18.8278 46degree: 148 (main wave) 48degree: 94.58; 50degree: 37.66 94degree: 67.5; 96degree: 71.76	22degree: 2.47% 23degree: 0.874 T (main wave) 25degree: 10.68% 71degree: 23.69%; 73degree: 11.37%	22degree: 2.47% 23degree: 0.889T (main wave) 25degree: 10.95% 71degree: 23.81%; 73degree: 11.42%
48-slot 50-pole	2degree: 16.85 46degree: 36.8; 48degree: 91.75 50degree: 141.87 (main wave) 96degree: 70.15; 98degree: 66.8	25degree: 0.8642 T (main wave) 23degree: 9.1%; 26degree: 2.42% 71degree: 12%; 73degree: 24%	25degree: 0.8731 T (main wave) 23degree: 9.3%; 26degree: 2.4% 71degree: 12.2%; 73degree: 24.3%
48-slot 52-pole	4degree: 19.8 44degree: 36.55; 48degree: 89.58 52degree: 139.24 (main wave) 96degree: 71.03; 100degree: 66.31	26degree: 0.8558 T (main wave) 22degree: 9.34%; 25degree: 2.63% 70degree: 11.8%; 73degree: 2.02% 74degree: 24%	22degree: 10.07% 25degree: 2.62% 26degree: 0.8755T(main wave) 27degree: 2.62% 70degree: 11.99% 74degree: 22.98%

and harmonic proportion of no-load air gap magnetic density can be seen in Table 2. According to the table, no-load main wave (22th order) of the 44-pole motor has high magnetic density (about 0.9T), and contains fewer lower order harmonics.

Fig. 3 shows harmonics distribution of air gap magnetic density under rated load, and harmonic proportion can be seen in Table 2, from which we can see that magnetic density main wave(22th power)of 44-pole motor is the highest (about 0.88T), and other lower order harmonics have smaller magnetic density.

3.2 Electromagnetic force calculation under different slot-pole combination

Radial and tangential component of air gap magnetic density in the four motors are calculated by FEM, and radial electromagnetic force is calculated based on expression (1). Fig. 4 shows harmonic distribution of radial force in four motor under rated load. Every harmonic proportion of radial force can be seen in Table 2.

From the Table 2 we can see that compared with 44-pole and 52-pole motor, 46-pole and 50-pole motors contain

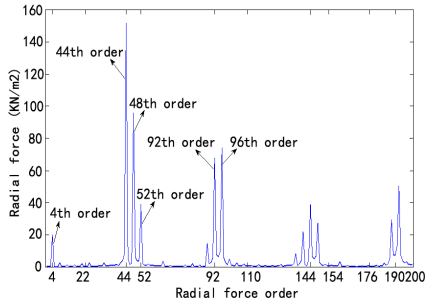

(a) 48-slot 44-pole motor

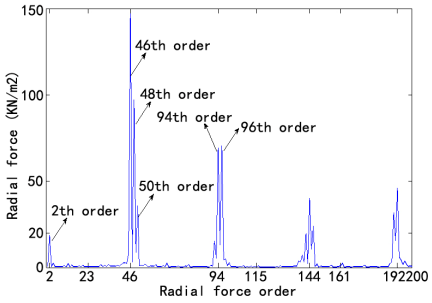

(b) 48-slot 46-pole motor

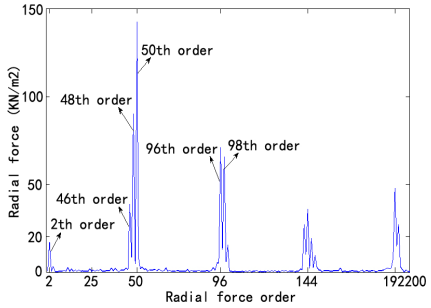

(c) 48-slot 50-pole motor

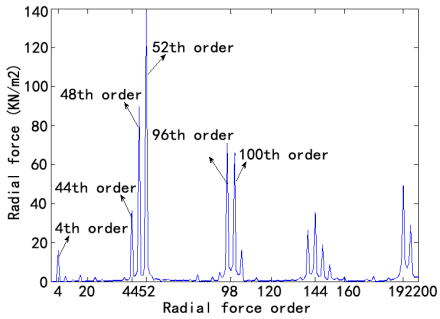

(d) 48- slot 52-pole motor

Fig. 4. Radial electromagnetic force of rated load motors

lower order force, which may cause more intense electro-magnetic oscillation. Besides, the latter ones apparently have more low order force.

As a conclusion, motor with slot-pole match of 48/44 has the smallest electromagnetic oscillation.

Table 3. Parameters of 6-phase fractional slot concentrated winding permanent motor

parameter	value	parameter	value
Rated power	20kW	Serial conductors per phase	128
Rated line voltage	380V	Rated torque	637 N·m
Pole-pairs	22	Rated phase current	17A
slot	48	Rated speed	300r/min
Stator external diameter	400mm	B_{s0}	2.5mm
Stator inner diameter	330mm	B_{s1}	8mm
Rotor external diameter	327mm	B_{s2}	12mm
Minimum air gap	1.5mm	H_{s0}	1mm
Iron core length	255mm	H_{s2}	23mm
Conductors per slot	32	H_{s1}	1mm
PM max height	5.7mm	Pole bias distance	120mm
Pole arc coefficient	0.83	Stator yoke height	10mm
Stator electro-density	4.79A/mm^2	Polar distance	23.56mm
Stator cogging distance	21.6mm	Parallel branches	1

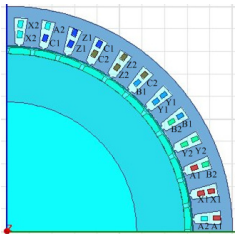

Fig. 5. Winding assignment of the motor prototype

(a) stator structure

(b) single PM

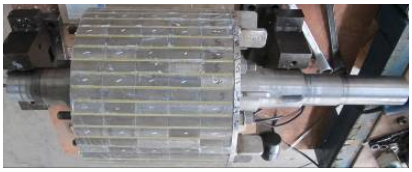

(c) rotor structure

(d) motor end

(e) motor appearance

Fig. 6. Structure of the prototype motor

4. 6-phase fractional-slots concentrated- winding PM motor design

According to analysis above, motor with slot-pole match of 48/44 is designed and manufactured. The basic

parameters are displayed in Table 3.

The stator slots are half close, and magnet material is N35UH. Modeling and calculations are based on Ansoft software, and distribution of windings is shown in Fig. 5.

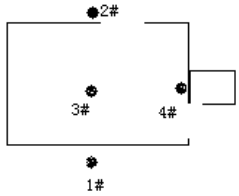

Fig.7. Sketch map of the oscillation measuring point

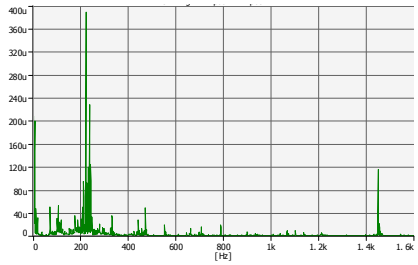

(a) no.1 measure point

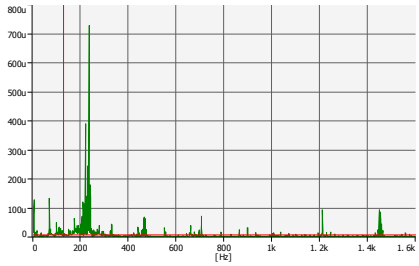

(b) no.2 measure point

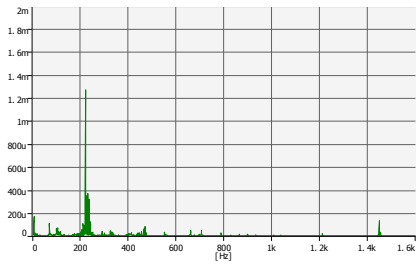

(c) no.3 measure point

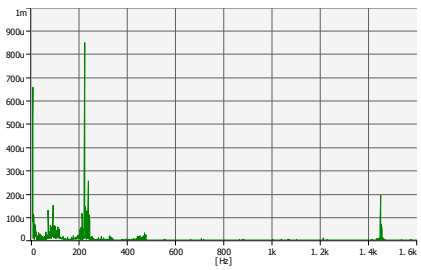

(d) no.4 measure point

Fig. 8. Acceleration distributions in frequency spectrum of motor under 300rpm

Prototype is manufactured according to electromagnetic calculation. In order to reduce eddy current in permanent magnet, permanent magnets are divided into 10 equal portions along axial direction and 5 equal portions along circumferential direction.

5. Experiments

Motor's structure is shown in Fig. 6. The motor is placed on test-bed, and four measurement points with acceleration sensor are attached on motor as shown in Fig. 7. The No.1 and No. 2 points are placed on the bottom of motor, and No. 3 and No.4 are on the top of motor. Besides, switching frequency of the 6-phase inverter is 2kHz. In the condition of rated speed (300r/min, 110Hz) and rated load, acceleration values in every point are measured.

Fig. 8 shows acceleration values of different frequencies obtained from four measurement points. According to the picture, oscillation acceleration comes to its maximum under quadratic input electric frequency, and the second point is close to 1450Hz (corresponding to motor's 4^{th} order force wave frequency).

6. Conclusion

A 6-phase fractional-slot concentrated-winding permanent magnetic motor is studied under no load and load status, as well as four possible slot–pole matches including 48/44, 48/46, 48/50 and 48/52. Its air-gap magnet field and radial electromagnetic force are both calculated.

It is concluded that, when the slot number is close to the pole number, lower-order radial electromagnetic force will be generated and electromagnetic oscillation will be enhanced. In the four motor design schemes proposed in this paper, motors with 48/46 and 48/50 slot-pole match generate 2th order radial force with high amplitude, and motors with 48/44 and 48/52 slot-pole match has 4th rather than 2th order force, and oscillation characteristic of the latter two motors are significantly better than the former two. Moreover, amplitude of the low-order radial force in 44-pole motor is less than that in 52-pole motor. So the final choice is 48/44 match. A 6-phase fractional-slot concentrated winding PM synchronized motor is designed and manufactured, and its experimental testing is accomplished as well.

Acknowledgements

This work was supported by the National Science Foundation of China. (51277177, 51007094)

References

[1] Patel. B. Reddy, Ayman. M. EL-Refaie, et al. Effect of number of layers on performance of fractional-slot concentrated-windings interior Permanent magnet machines. *8th International Conference on Power Electronics - ECCE Asia*, 2011, 3:1921-1928.

[2] Lei Hao, General Motors Warren. Design and analysis of IPM machine with bar wound fractional slot distributed winding for automotive traction application. *Energy Conversion Congress and Exposition* (*ECCE*), 2013:598-605.

[3] Aldo Boglietti, Ayman M, Oliver Drubel, et al. Electrical machine topologies hottest topics in the electrical machine research community, *IEEE industrial electronics magazine*, 2014(6):18-30.

[4] E. A. Klingshirn. High phase order induction motors — Part I — description and theoretical considerations, *IEEE Trans. Power App.Syst*., 1983,102, (1): 47-53.

[5] E.Levi. Multiphase electric machines for variable-speed applications. *IEEE Trans. Ind. Electron.* 2008, 55(5):1893-1909.

[6] L. J. Wu, Z. Q. Zhu, J. T. Chen, Z. P. Xia, Optimal split ratio in fractional-slot interior permanent-magnet machines with non-overlapping windings. *IEEE Tractions on Magnetics*, 2010, 46(5): 1235-1242.

[7] Massimo Barcaro, Adriano Faggion, Nicola Bianchi. Sensorless rotor position detection capability of a dual three-phase fractional-slot IPM machine. *IEEE Transactions on Industry Applications*, 2012, 48(6): 2068-2078.

[8] Haodong Yang, Yangsheng Chen. Influence of radial force harmonics with low mode number on electro-magnetic vibration of PMSM. *IEEE Trans. on Energy Conversion*, 2014, 29 (1)38-45.

[9] Mohammad Islam, Rakib Islam, Tomy Sebastian. Noise and vibration characteristics of permanent magnet synchronous motors using electromagnetic and structural analyses. *Energy*: 3399-3405

[10] YU Pei-qiong, Liu Sheng. Techniques for reducing the effects of detent force in ' PMLSMs. *International Conference on Computational Electromagnetic and Its Applications Proceedings*, 2004:126-129.

[11] Y. S. Chen, Z. Q. Zhu, D. Howe. Vibration of PM brushless machines having a fractional number of slots per pole. *IEEE Trans. on Magnetics*, 2006, 42(10): 3395 - 3397

[12] Sun-Kwon Lee, Gyu-Hong Kang, Jin Hur. Finite element computation of magnetic vibration sources in 100 kW two fractional-slot interior permanent magnet machines for ship. *IEEE Trans. on Magnetics*. 2012, 48(2):867-870.

[13] Van Li, Shuangpeng Li, Jiakuan Xia, Fengge Zhang. Noise and vibration characteristics analysis on different structure parameters of permanent pagnet synchronous motor. *International Conference on Electrical Machines and Systems*, 2013:46-49.

Qiao Ming-zhong He is a professor in Naval University of Engineering, Wuhan 430033, Hubei Province, China. His research interests are power system automation and ship propulsion motor.

Zhu Yong-xin He is a Ph.D. student in Naval University of Engineering, Wuhan 430033, Hubei Province, China. His research interests are power electronics and ship propulsion motor.

Liang Jing-hui He is a Ph.D. student in Naval University of Engineering, Wuhan 430033, Hubei Province, China. His research interests are motor design and multi-field coupling.

Li Geng He is a Ph.D. student in Naval University of Engineering, Wuhan 430033, Hubei Province, China. His research interests are motors and electric machines.